ELSEVIER

Materials Science and Engineering A348 (2003) 208–216

MATERIALS SCIENCE & ENGINEERING A

www.elsevier.com/locate/msea

Neutron diffraction study of the deformation behaviour of deformation processed copper–chromium composites

K.L. Lee [a,*], A.F. Whitehouse [a], P.J. Withers [b], M.R. Daymond [c]

[a] *Department of Engineering, University of Leicester, University Road, Leicester LE1 7RH, UK*
[b] *Manchester Materials Science Centre, Grosvenor St., Manchester M1 7HS, UK*
[c] *ISIS Facility, Rutherford Appleton Laboratory, Chilton, Didcot, Oxon OX11 0QX, UK*

Received 5 May 2002; received in revised form 19 September 2002

Abstract

The tensile behaviour of a co-deformed Cu–10vol.% Cr composite has been studied. The composite was produced from cast Cu–Cr by hot forging and then cold swaging to a reduction of 95.6% in order to attain a fibrous reinforcing microstructure. Tensile testing in situ on a neutron diffractometer has allowed the evolution of axial and transverse elastic strains in each phase to be monitored as a function of applied stress. The results show that contrary to expectation, inelastic load transfer occurs from the Cr to the Cu matrix. The measured elastic strains are compared with an Eshelby type model and the retained misfit between the phases calculated. Since damage of the fibres, even near the fracture surface was limited, it is inferred that load transfer to the matrix occurs by the greater relative plastic straining of the reinforcement.

Keywords: Cu–Cr in situ composite; Neutron diffraction; Eshelby; Load sharing

1. Introduction

In view of the mediocre mechanical properties of relatively pure, highly conducting copper alloys there is interest in developing copper matrix composite materials for electrical applications. Ideally, the reinforcing phase should be fibrous to achieve optimal mechanical properties without seriously compromising conductivity. Composites based on metallic reinforcements have the advantages of some conductivity in the second phase as well as having ductile characteristics. Three approaches have been followed; the incorporation of metallic fibres (e.g. Cu–W [1]), eutectic composites in which the second phase is produced in situ (e.g. Al–Al_3Ni [2], Cu–1.56%Cr [3]), and deformation processed materials (e.g. Cu–20%Nb [4], Cu–15 vol.% Cr [5]). Composites based on including fine wires tend to be rather expensive to produce, whereas, eutectic composites are restricted to eutectic compositions and chemistries (e.g. only 1.56% Cr reinforcement for Cu–Cr). Composites formed by co-deformation can be produced fairly cheaply with variable volume fractions [6–10]. Research has shown that co-deformed copper-based composites give significant improvements in strength, while maintaining good thermal and electrical conductivity [7]. It has been established that the incorporation of a bcc metal reinforcement such as Nb, Cr, Fe and V within the fcc copper matrix is particularly advantageous [8–12]. The bcc structure results in the development of a ribbon-like reinforcing morphology within the Cu matrix during the deformation.

To date, considerable research has been carried out to optimise the mechanical and electrical properties of Cu–Cr composites [13,14]. However, experimental evidence is lacking on the load partitioning between the two phases under applied loading. In a conventional MMC, deformation in the matrix causes a misfit to be generated between the matrix and the plastically non-deformable reinforcement. However, Cu–Cr composites differ fundamentally from conventional composites in that both phases are able to deform plastically [15]. Therefore, the amount of load transfer is determined by

* Corresponding author. Current address: 8 Pope Street, Knighton Fields, Leicester, LE2 6DX, UK. Fax: +44-116-252-2525
E-mail address: kokloong1@hotmail.com (K.L. Lee).

0921-5093/02/$ - see front matter
PII: S0921-5093(02)00688-3

the relative extent of elastic and plastic deformation in each phase, and this in turn depends on the dominant deformation mechanism operating in each phase at a given temperature. The composite is considered efficient if a high proportion of the applied load is carried by the reinforcing phase. The load-partitioning ratio of an applied load between the matrix and reinforcement will normally remain constant with increasing load if both phases remain elastic. However, this ratio will change if one or both of the phases starts to deform plastically. Besides strengthening by load partitioning, microstructural strengthening can occur because of the refinement of microstructure and the introduction of plastic work introduced during the co-deformation processing stage.

The purpose of the current research was to understand the deformation behaviour of the individual phases in a high reinforcing volume Cu–Cr composite and their interaction through elastic and plastic loading at room temperature. Our approach has been to follow the deformation behaviour of the individual phases by neutron diffraction. The advantage of neutrons over X-rays is that the high level of penetration, even in relatively heavy elements such as Cu (attenuation length ~ 10 mm), mean that the performance of each phase can be monitored in the bulk non destructively [16]. This technique has been used extensively to study thermally and mechanically induced strains in a number of composites [17–22]. The diffraction method is sensitive only to the elastic component of strain and thus the recorded strains can be related to the stress in each phase. From the load partitioning between phases inferences can be made on the effects of plasticity on the total deformation.

2. Neutron diffraction method of strain measurement

The time-of-flight (TOF) neutron diffraction method has been used for strain measurement. A pulsed beam of polychromatic neutrons is incident upon the sample and the diffracted spectra are measured by detectors at fixed angles as a function of wavelength. The wavelength is determined by recording the TOF and thereby the velocity of each detected neutron. Our experiments have been carried out on the ENGIN instrument at ISIS, Rutherford Appleton Laboratory where 2θ is fixed at $\pm 90^\circ$ and λ varies with time. The technique exploits the lattice spacings as an atomic strain gauge. Their spacings are derived from the shifts in the diffraction peaks using Bragg's Law:

$$\lambda = 2d_{hkl} \sin \theta_{hkl} \tag{1}$$

where λ is neutron wavelength, 2θ the scattering angle and d_{hkl} the lattice spacing between the (hkl) planes. The wavelengths of the detected neutrons are calculated using the de Broglie equation:

$$\lambda = \frac{h}{m_n v} = \frac{ht}{m_n L} \tag{2}$$

where h is Planck's constant, m_n the neutron mass (1.675×10^{-27} kg), v the neutron speed, L the total length of the flight path of the neutron (source to sample to detector) and t is the recorded time of flight. By combining Eqs. (1) and (2), the d-spacing can be expressed in terms of the time of flight as:

$$d_{hkl} = \frac{ht}{2m_n L \sin \theta_{hkl}} \tag{3}$$

Elastic strains for individual lattice planes are then calculated using:

$$\varepsilon_{hkl} = \frac{\Delta d_{hkl}}{d_{ohkl}} \tag{4}$$

where Δd_{hkl} is the change in the stress-free lattice spacing Δd_{ohkl}. In actual fact this shift is measured as a time shift in the peak. Each pulse of neutrons produces a diffraction profile containing many peaks, which is normally added to subsequent pulses until the total intensity is great enough to give a statistically meaningful measurement of lattice spacing.

Rather than focus on the time shift for a single hkl peak, it is more efficient to use a, Rietveld or Pawley refinement [23] to refine (determine) the lattice parameter. Besides being more efficient, because information from different diffraction peaks is combined to establish the most representative change in lattice parameter, the result is usually less sensitive to elastic and plastic anisotropies [24]. These can make the shift for any given hkl unrepresentative of the bulk polycrystalline averaged (engineering) response.

3. Experimental procedures

3.1. Materials

Cu–10 vol.% Cr co-deformed composite was produced by vacuum casting at 1600 °C by Essex Metallurgical Limited. It was then forged at 900 °C and swaged at room temperature into 3 mm diameter rod, with a final reduction in area of 95.6%. Prior to forging and swaging, the Cr is in a dendritic form as shown in Fig. 1a. During subsequent high deformation, the dendrites elongate into fibres with a mean thickness of 2 μm. Since the original Cr dendrites form a quasi-continuous structure, the final Cr fibres can be classified as continuous reinforcement (Fig. 1b). The fibre aspect ratio is about 25 and the Cu grain size very small. The elastic properties of the two phases are taken to be those given in Table 1.

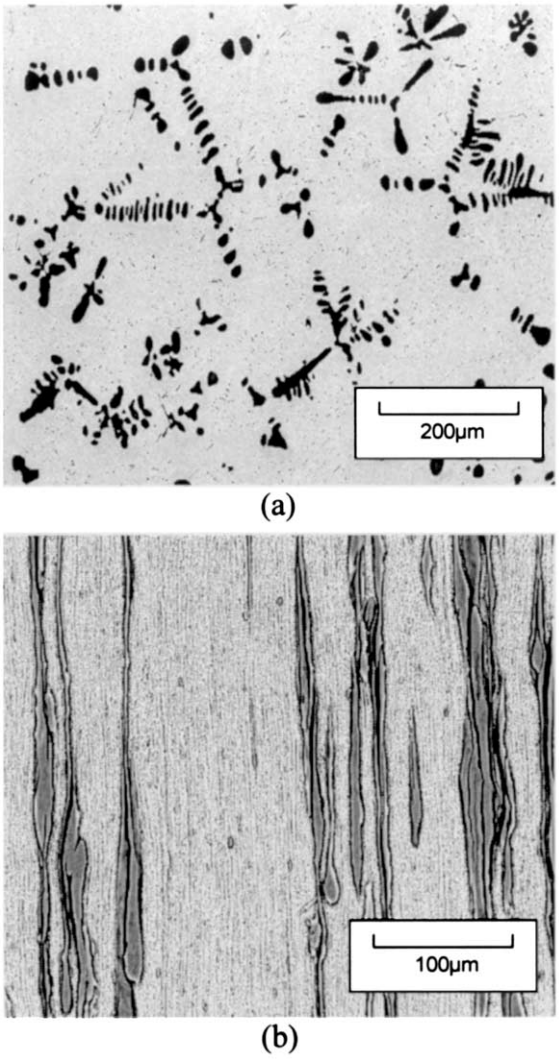

Fig. 1. (a) SEM image of the as-cast composite, the Cu matrix having been selectively etched away and (b) a BE image of the as-drawn co-processed composite.

3.2. Microstructural analysis

Fractured specimens were mounted in resin and then ground to a depth equivalent to about half of the diameter of the specimen using SiC papers to reveal the maximum longitudinal section of the cylindrical rods. The metallographic surfaces of the longitudinal sections were prepared using the standard procedure of grinding and polishing. The fracture surfaces of the specimens were examined by scanning electron microscopy (SEM). About 40% HNO_3 was used to deep etch the specimen for the SEM observations. In this way, a layer of Cu could be removed while leaving the Cr fibres visible thus revealing any microstructural damage.

3.3. In situ neutron diffraction loading experiment

Details of the experimental set-up can be found elsewhere [25] and hence they are only summarised briefly here. A hydraulic tensile testing machine was installed on the diffractometer table at ENGIN. Room temperature tensile tests were performed using incremental step loads in order to maximise the data obtained on a single sample during limited neutron beam time. While the neutron measurements were made the sample was held under load control, after which the load was then raised to the next level of stress. An extensometer was attached to the specimen to record macroscopic strain during the experiment.

Tensile test-pieces were 70 mm long with a circular cross section and a diameter of 3.09 mm. The loading axis was horizontal and at 45° to the incoming beam. This meant that the two 90° detectors were able to measure the lattice plane spacings parallel to and perpendicular to the tensile axis simultaneously. A schematic diagram of the experimental set-up is shown in Fig. 2. The stress levels chosen for this experiment were 5, 100, 250, 350, 375, 400 and 415 MPa and the stress–strain curve is shown in Fig. 3. In order to ensure that the specimen was properly aligned, a nominal stress

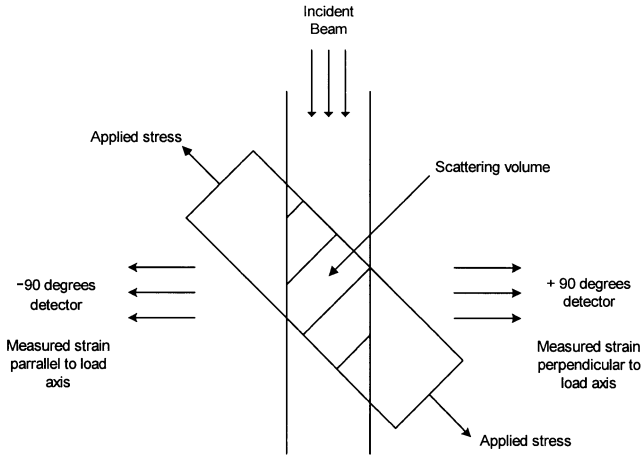

Fig. 2. Schematic of experimental set-up.

Table 1
Typical elastic, coefficient of thermal expansion (CTE), and plastic properties of the two phases

Volume fraction	Poisson's ratio	Young's modulus (GPa)	CTE (με K^{-1})	Bulk UTS (MPa)
0.90	0.34	135	16.5	280
0.10	0.21	280	6.5	690

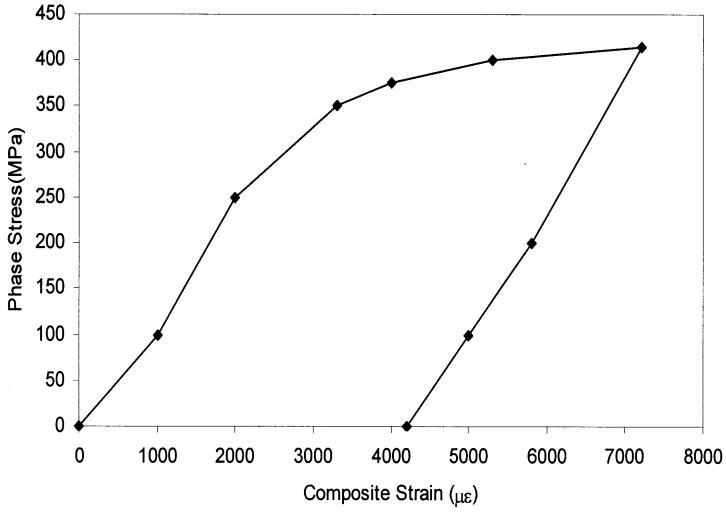

Fig. 3. The composite straining response during the tensile test on the neutron diffractometer. The points correspond to the positions at which neutron measurements were made (~4 h per point).

of 5 MPa was used for the initial unloaded measurement and this was taken as the 'zero point' of the experiment. A count time of approximately 4 h was needed to give adequate counting statistics in the diffracted spectra for both phases at each stress level. Due to the relatively poor diffraction signal from the small volume fraction of the Cr, the uncertainties in strain are much larger than in Cu phase.

4. Results

4.1. Deformed microstructures and fractography

The composite exhibited a highly ductile fracture. Limited damage was seen in the vicinity of the fracture surface as shown in Fig. 4b. The fracture surface Fig. 4a shows a combination of fine and coarse dimples. It can be seen clearly that Cr fibres lie at the bottom of each of the ductile dimples. The longitudinal cross section taken near the fracture surface shown in Fig. 4b suggests that fibre fracture is not extensive, even at very high strains, but voids near the fibre ends can form at high strains.

4.2. Neutron diffraction

The measured axial lattice strains are shown as a function of the applied load in Fig. 5a and the concomitant transverse strains are shown in Fig. 5b. The presence of thermal or process induced strains have been neglected in the figure by plotting the lattice strains relative to the lattice parameter measured at 5 MPa prior to testing. A number of features are immediately apparent. Firstly, the statistical quality of the matrix peaks (typical strain uncertainties ± 20 με (1 με = 10^{-6})) are far superior to those for the fibres (± 200

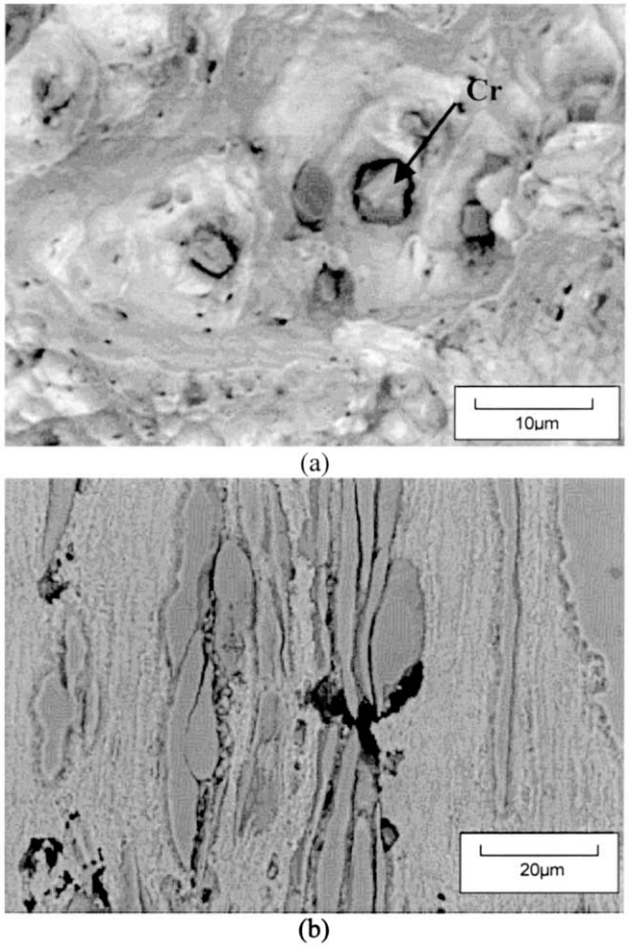

Fig. 4. (a) SEM image of a typical fracture surface of the composite tested at room temperature (b) longitudinal section near the fractured end.

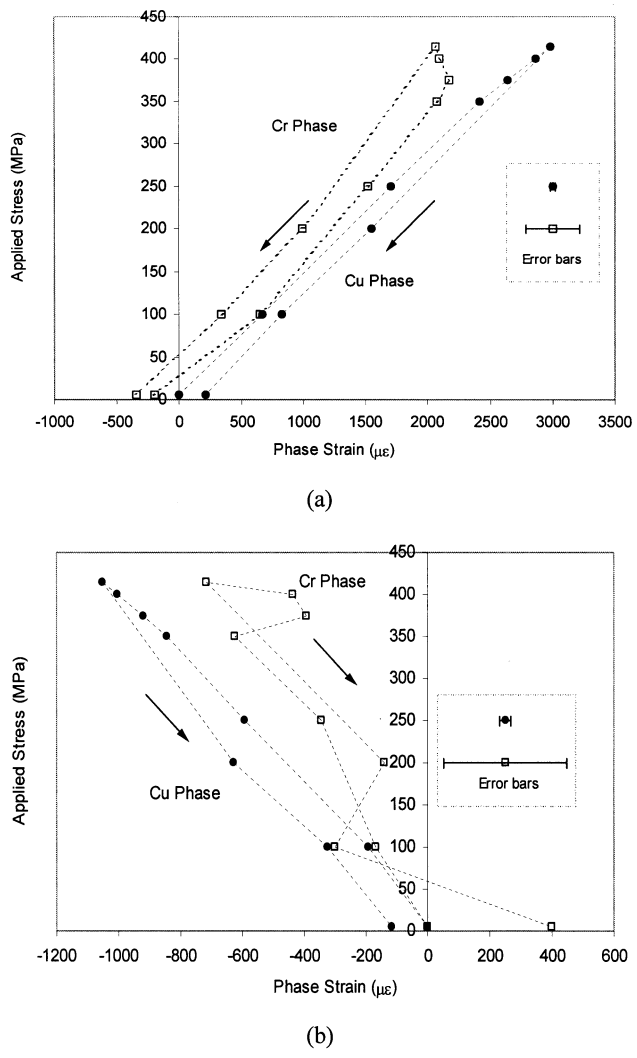

Fig. 5. Cu matrix and Cr fibre Pawley refined lattice strains as measured by neutron diffraction in the (a) axial and (b) transverse directions. The strains are shown relative to the initial nominally unloaded case (actually 5 MPa). The arrows indicate the unloading path.

με) in both the axial and transverse directions. Considering the axial response first, the Cr phase appears to strain to a larger extent than the Cu in the early stages of straining. Given the large aspect ratio of the fibres, a simple equal strain model would be expected to be sufficient for the elastic regime with the result that one would expect the Cu and Cr strains to be equal in the early stages of straining. Given the uncertainties in the measurements it is possible that the strain free reference for the Cr phase is in error. Indeed, an offset of around −200 με (i.e. within the measurement error) in the strain-free lattice parameter would bring the Cr phase at all times equal or below the elastic strain in the more compliant Cu phase in agreement with expectations[1]. It is clear that the copper curve begins to deviate from linearity at about 250 MPa, which corresponds to the onset of macro plasticity in the composite response (Fig. 3). At around 350–375 MPa significant load transfer is evidenced by the increasing elastic strains in the Cu phase and the sudden decrease in the rate of loading of the Cr. This result is perhaps contrary to expectation, given the larger yield stress typical of fine Cr fibres/ribbons compared with Cu (Table 1). The presence of tensile matrix final residual strains and compressive fibre strains are indicative of a positive misfit between the fibres and the matrix, in that the stress-free shape of the Cr inclusions appears to be longer than the 'holes' in which they sit. Such a plastic misfit causes an inelastic transfer of load from Cr to Cu. Load transfer from fibres to matrix during loading could also occur by matrix voiding (or fibre fracture), but these would not of themselves give rise to residual stresses.

[1] Note that this could also be achieved if the first loaded point were in error by 200 με, but this gives less good agreement overall (Fig. 6).

5. Discussion

In order to interpret the results in terms of load transfer it is helpful to use some form of model. In this paper we have used a development of Eshelby's elastic inclusion model, which is well suited to the study of fibrous composites [26]. Because of the fibrous morphology other models would also give similar results. Internal stresses arise from misfits, which can originate elastically, plastically or thermally. To calculate these we have used the elastic properties summarised in Table 1. The stiffness of the Cu matrix used here is slightly higher than the normal isotropic bulk value because of the texture generated by the swaging process. To conserve volume, the retained plastic misfit strain vector ε^{P*} between the phases was taken to have the form $\varepsilon^{P*}(-1/2, -1/2, 1)$ with the three-axis parallel to the loading direction, with a positive ε^{P*} indicative of a greater axial tensile strain in the Cr than the Cu. The elastic response was calculated solely on the basis of the elastic properties of the phases and the fibre aspect ratio. The variation in the retained matrix-fibre misfit generated during plastic straining was chosen so as to mimic the axial Cu matrix strain response. The transverse Cu, longitudinal and transverse Cr strains then follow automatically once the misfit has been established and are shown in Fig. 6. The misfit strains thus determined are shown in Fig. 7 and indicate that the Cr extends plastically to a greater extent than the Cu. The rate of misfit generation increases at a decreasing rate as the composite strains plastically. These misfit strains are at no stage sufficient to bring about the observed plastic strain without some plastic strain in the Cu. The elastic and plastic partitioning of strain (the large aspect ratio of the Cr fibres (ribbons) means that the total strains in each phase are nearly equal) is shown in Fig. 8. For

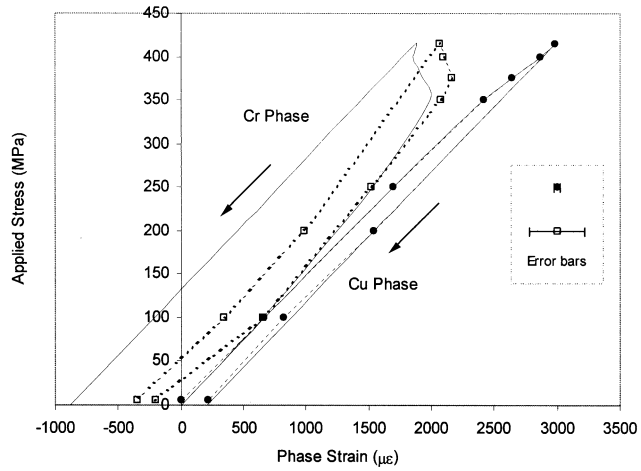

(a)

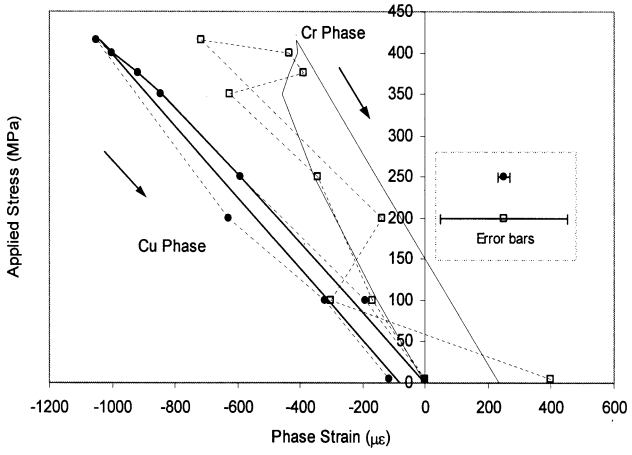

(b)

Fig. 6. Cu matrix and Cr fibre lattice strains measured by neutron diffraction and as predicted by the Eshelby model (solid line) in the (a) axial and (b) transverse directions using the misfits shown in Fig. 7. In (a) the Cr strains have been offset by −200 microstrain (less than the measurement error). The arrows indicate the unloading path.

example when the misfit between the phases is 1000 με and the composite plastic strain is around 2540 με (corresponding to a total composite strain of ~5300 με), the extension of the composite caused solely by this misfit is only around 200 με (volume fraction × equivalent homogeneous stress-free misfit strain). In other words the plastic strains in the two phases are 2440 and 3440 με for the Cu and Cr phases, respectively, as illustrated in Fig. 8. The plateaux in Fig. 7 indicates that, at the higher plastic strains the two phases deform more and more similarly. Alternatively the misfit may be being relaxed either plastically (unlikely given the large aspect ratio) or through the occurrence of damage however the latter mechanism alone would not explain the observed residual strains. Indeed some degree of co-

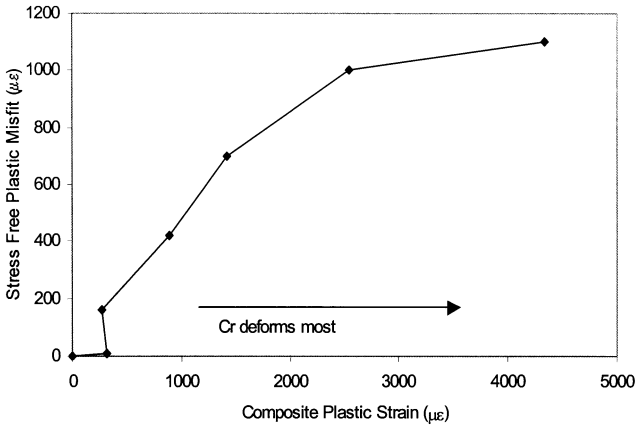

Fig. 7. The stress free fibre-matrix misfit (a positive strain indicates the Cr to be strained more than the Cu) inferred from the axial inelastic lattice strain response of the Cu phase.

deformation is consistent with the increase in aspect ratio observed with increasing drawing strain [27].

The axial and transverse phase strains calculated on the basis of the misfit plotted in Fig. 7 are shown in Fig. 6. As it must, the modelled axial Cu response is in good agreement with the data. More importantly, the overall shape of the axial Cr response is well predicted, even if the final residual compressive strain is overestimated (this is probably due to an overestimation of the Cr ribbon Young's modulus, but could also be due to the influence of limited damage). In the transverse direction the agreement with the measured data is within the errors of the measurements, with the compressive Cu and the tensile Cr residual strains well predicted. Given the good agreement with the measured strains it is worthwhile plotting the inferred phase stresses (Fig. 9). At low loads the elastic curves lie below the expected elastic response (see also Fig. 8). This is thought to be due to an overestimation of the composite strain caused by a small amount of bending of the sample recorded by the clip gauge during the early stages of loading. Unfortunately, in order to allow unfettered access to the sample by the neutron beam it was not possible to attach two diametrically opposing clip gauges to overcome this effect.

Note that the phase stresses shown in Fig. 9 represent the changes relative to the initially unloaded state. They therefore do not include pre-existing residual stresses. It is clear from the Fig. 9 that the stresses increase in the Cr phase by about 500 MPa and then saturate while the Cu phase begins to plastically deform when the phase stress has increased by about 330 MPa, saturating at around 400 MPa. At first glance it is surprising that the Cr deforms preferentially in view of the very high load bearing capacity of Cr fibres established from other work (8 GPa for 0.4 μm fibres down to 2 GPa for 1.2 μm fibres [28]). However, since the mean fibre diameter is ~2 μm a yield stress below 1 GPa is not unreasonable

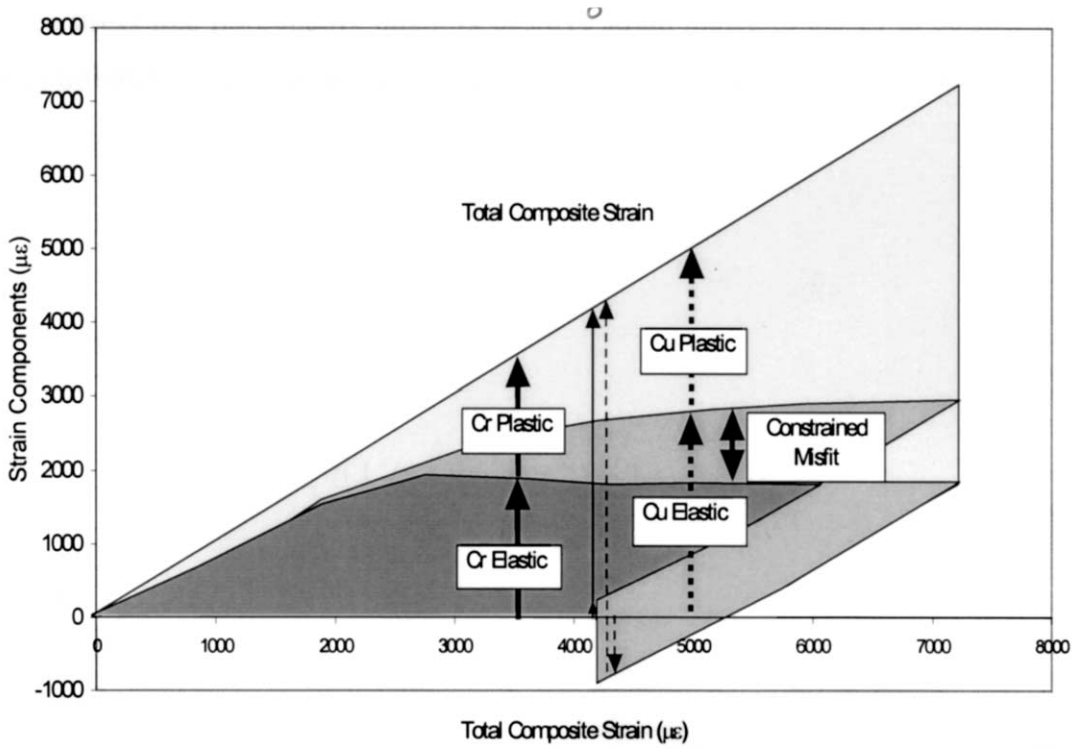

Fig. 8. The elastic and plastic partitioning of strain for each phase. Note that the constrained misfit shown here is slightly less than the stress-free misfit shown in Fig. 7 because the fibres are not infinitely long. The elastic strain in the fibres appears to saturate soon after the onset of yielding due to insufficient work hardening so that the Cr elongates plastically further than the matrix, which extends by a combination of elastic and plastic straining. The bold arrows indicate the contributions under load, the thin after unloading.

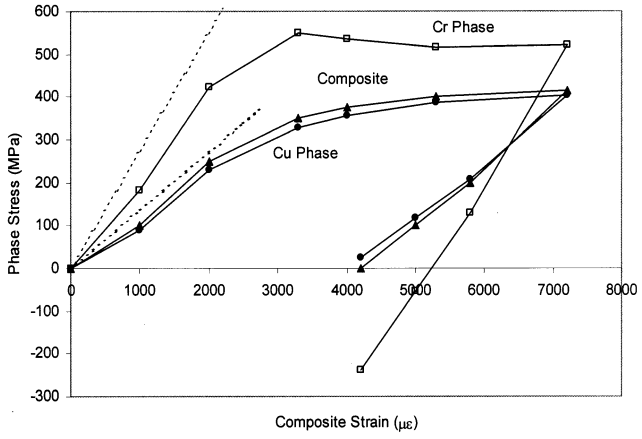

Fig. 9. The individual Cu (circles) and Cr (squares) axial phase stress responses compared with the bulk composite (triangles) response. The stiffness of single phase Cu and Cr are shown by the dashed lines.

and a value of ~690 MPa quoted in Smitthells for bulk drawn Cr may not be unrealistic. When considering these results it is worth remembering that the composite was heavily co-deformed prior to tensile testing. This has increased the aspect ratio of the fibres, introduced considerable plastic strain into both phases and probably generated considerable residual strains.

Sun [27] asserts that for co-deformation during composite manufacture the flow stress of the copper must be greater than or at least equal to that for the Cr phase. This is not actually true; rather the Cr must be brought to and maintained at its yield locus as the Cu is progressively deformed. Initially, the dendritic Cr can be brought to its yield locus by a mixture of elastic and plastic misfit. Provided plastic relaxation is not too severe plastic deformation of a matrix can transfer load towards a non deforming phase very effectively (e.g. [29]) even for globular morphologies. As the fibres increase in aspect ratio, loading of the Cr becomes more effective. Previous work [27] has indicated that for Cu–15%Cr tensile residual stresses of ~140 MPa were generated by drawing to a strain of 3.1. Such stresses would be balanced by a compressive stress of around −16 MPa in the Cu phase. In our own lab X-ray experiments: we were not able to measure self-equilibrating residual stresses, but instead recorded compressive stresses in both phases, possibly due to macroresidual stresses caused by swaging. If the results of Sun are applicable to our composite then this would mean that the Cr yield stress exhausts at a value approaching 700 MPa. A relatively low Cr yield stress combined with tensile Cr phase residual stresses would also explain the relatively poor performance of the composite here relative to the Cu–15 vol.% Cr composites of Adachi et al. [5] (composite UTS 900 MPa). In this context it should also be remembered that each

neutron measurement took around 4 h to complete so that, at high strains at least, deformation occurs at lower stresses ($\sigma_{uts} \sim 415$ MPa) than for a conventional strain-rate tensile test ($\sigma_{uts} \sim 440$ MPa) [30].

Funkenbusch and Courtney [31] suggested that the Cu phase would have work hardened according to:

$$\sigma_{ys} = 228 + 156\varepsilon^{0.24} \text{ MPa} \quad (5)$$

with ε representing the true Cu strain. This would suggest a value of around 430 at a strain of 3.1. This is somewhat higher than the Smitthels reference value (Table 1) or our own value (~ 280 MPa) evaluated from a tensile test. These later values are more in line with our inferred response both without (Fig. 9) and with the initial residual stresses (~ -16 MPa) superimposed.

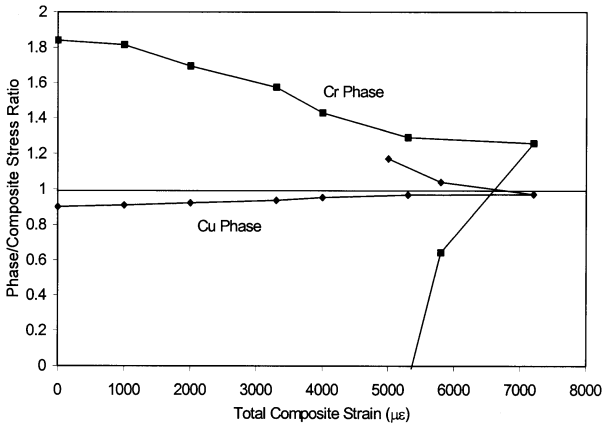

Fig. 10. The ratio of the phase stress to the composite stress for the two phases as a function of the total composite strain.

6. Conclusions

It has been possible to measure the changes in elastic strain with applied tensile loading by neutron diffraction in the axial and transverse directions for the Cu and Cr phases in a Cu–10 vol.% Cr co-deformed composite. As expected given the aspect ratio of the Cr fibres, in the elastic regime the two phases strain almost equally in the axial direction. Perhaps contrary to expectations however, the onset of plasticity results in a strain misfit between the phases, which acts to transfer load towards the Cu phase. Since damage in the Cr phase during straining is not significant in common with earlier observations [32], it must be concluded that the Cr phase deforms more than the Cu phase. This is borne out by the final residual strains. This is because co-deformation prior to testing has meant that the Cr phase reaches the yield locus at approximately the same strain as the Cu phase. This is due to a combination of its higher stiffness and the probable presence of swaging induced residual stresses. A flatter work hardening rate for the Cr phase relative to the Cu phase means that although the two phases deform approximately equally, the Cr phase has the larger plastic component resulting in load transfer from Cr to Cu with increased straining. This is evident in Fig. 10 which shows that while the Cr phase is effective in bearing a greater proportion of the load in the elastic regime, this advantage decreases with increased plastic straining decreasing to just 20% greater than the applied load at a strain of 0.7%. This plot also illustrates that even at its best (in the elastic regime) the stress in the Cu phase is only 10% less than the applied load from which it is clear that microstructural refinement and worked microstructures are at least as important as load transfer for the improving the mechanical performance of this system. A better tensile performance might be expected if the damaging tensile residual stresses could be relieved prior to tensile testing without softening either phase significantly. Of course considering elevated temperature properties; thermal residual stresses would counterbalance the existing residual stresses giving an improvement in properties over that which would otherwise be expected.

Acknowledgements

The support of the EPSRC Network for Neutron and Synchrotron Strain Measurement is acknowledged. Thanks are also due to K.A. Roberts of Cambridge University Materials Science and Metallurgy Department and G.R. O'Connor of Leicester University.

References

[1] H.P. Cheskis, R.W. Heckel, Met. Trans. 1 (1970) 1931.
[2] F.D. George, J.A. Ford, M.J. Salkind (Eds.), Metal Matrix Composites STP 438, ASTM, Philadelphia, 1968.
[3] A.M. Russell, L.S. Chumbley, Y. Tian, Adv. Eng. Mater. 2 (2000) 11.
[4] W.A. Spitzig, P.D. Krotz, Acta Metall. 36 (1988) 1709.
[5] K. Adachi, T. Sumiyuki, T. Takeuchi, H.G. Suzuki, J. Jpn. Inst. Met. 61 (1997) 367.
[6] T.W. Ellis, I.E. Anderson, H.L. Downing, J.D. Verhoeven, Metalurgical Transactions 24 (1993) 21.
[7] W.A. Spitzig, H.L. Downing, F.C. Laabs, E.D. Gibson, J.D. Verhoeven, Met. Trans. A 24 (1993) 7.
[8] C. Biselli, D.G. Morris, Acta Mater. 44 (1996) 493.
[9] P. Liu, S. Bahadur, J.D. Verhoeven, Wear 166 (1993) 133.
[10] S.T. Kim, P.M. Berge, J.D. Verhoeven, J. Mater. Eng. Perform. 4 (1995) 573.
[11] A.R. Pelton, F.C. Laabs, W.A. Spitzig, C.C. Cheng, Ultramicroscopy 22 (1987) 251.
[12] C.L. Trybus, L.S. Chumbley, W.A. Spitzig, J.D. Verhoeven, Ultramicroscopy 30 (1989) 315.
[13] J.D. Verhoeven, W.A. Spitzig, F.A. Schmidt, P.D. Krotz, E.D. Gibson, J. Mater. Sci. 24 (1989) 1015.
[14] T.W. Ellis, S.T. Kim, J.D. Verhoeven, J. Mater. Eng. Perform. 4 (1995) 581.
[15] K.L. Lee, A.F. Whitehouse, A.C.F. Cocks, ICCM 12, 1999 Paris.

[16] P.J. Withers, Key Eng. Mater. Ceram. Matrix Compos. 108-110 (1995) 291.
[17] M.R. Daymond, C. Lund, M.A.M. Bourke, D.C. Dunand, Metal. Mater. Trans. A 30 (1999) 2989.
[18] M.R. Daymond, P.J. Withers, International Conference on Composite Materials 10, 1995, Whistler, Vancouver, Canada.
[19] D.H. Carter, M.A.M. Bourke, Acta Mater. 48 (2000) 2885.
[20] H.M.A. Winand, A.F. Whitehouse, P.J. Withers, Mater. Sci. Eng. A 284 (2000) 103.
[21] A.J. Allen, M. Bourke, S. Dawes, M.T. Hutchings, P.J. Withers, Acta Metall. 40 (1992) 2361.
[22] P.J. Withers, A.P. Clarke, Acta Mater. 46 (1998) 6585.
[23] H.M. Rietveld, Acta Crystallogr. 22 (1967) 151.
[24] M.R. Daymond, M.A.M. Bourke, R.V. Dreele, B. Clausen, T. Lorentzen, J. Appl. Phys. 82 (1997) 1554.
[25] M.R. Daymond, H.G. Priesmeyer, Acta Mater. 50 (2002) 1613.
[26] P.J. Withers, W.M. Stobbs, O.B. Pedersen, Acta Mater. 37 (1989) 3061.
[27] S. Sun, Metal. Mater. Trans. A 32 (2001) 1225.
[28] M.J. Salkind, F.D. Lemkey, F.D. George, in: A.P. Levitt (Ed.), Whisker Technology, Wiley-Interscience, New York, 1970, p. 343.
[29] T.W. Clyne, P.J. Withers, An Introduction to Metal Matrix Composites, Cambridge Solid State Series, 1993, p. 509.
[30] K.L. Lee, A.F. Whitehouse, P.J. Withers, Metal. Mater. Trans. A, submitted for publication.
[31] P.D. Funkenbusch, T.H. Courtney, Scr. Mater. 15 (1981) 1349.
[32] K.L. Lee, H.E. Carroll, A.F. Whitehouse, Mater. Sci. Technol. 16 (2000) 811.